The Reaction of Nitrogen Atoms with Methyl Radicals: Are Spin-Forbidden Channels Important?

Alvaro Cimas and Antonio Largo*

Departamento de Química Física, Facultad de Ciencias, Universidad de Valladolid, 47005 Valladolid, Spain

Received: June 6, 2006; In Final Form: July 10, 2006

A computational study of the $N(^4S) + CH_3$ reaction has been carried out. The reactants approach through an attractive potential surface leading to an intermediate, H_3CN, whose formation does not involve any barrier. In agreement with the experimental results, the dominant channel for this reaction is H_2CN+H. The theoretically estimated rate coefficient for the overall process at 298 K is 9.1×10^{-12} cm^3 s^{-1} molecule^{-1}, which is nearly 1 order of magnitude lower than the experimental result, but also much larger than those computed for the reactions of ground-state nitrogen atoms with halomethyl radicals. The analysis of the singlet potential energy surface, and the corresponding computational kinetic study, shows that for the reaction of excited nitrogen atoms with methyl radicals, the preferred product from the kinetic point of view is also H_2CN+H, but in this case production of HCN is significant (with branching ratios around 0.185). According to our calculations, spin-forbidden processes are highly unlikely for the $N(^4S) + CH_3$ reaction. However, further evolution of the preferred products, H_2CN+H, might explain the experimental observation of hydrogen cyanide as a minor product in this reaction.

Introduction

The reaction of ground-state nitrogen atoms with methyl radicals is interesting in different fields. It is believed to be a major source of hydrogen cyanide in the atmosphere of different planets, such as Titan and Neptune.[1,2] For example, the photochemical breaking of molecular nitrogen gives rise to both ground-state and excited nitrogen atoms[3] through the following process:

$$N_2 + h\nu \rightarrow N(^4S) + N(^2D) \qquad (1)$$

In addition, the reaction of nitrogen atoms with methyl radicals seems to play a significant role in the formation of HCN in circumstellar clouds.[4] Consequently, it has considerable relevance in astrochemistry. Furthermore, it is also thought to be important in combustion processes[5,6] and in the reactions of nitrogen atoms with hydrocarbons.[5]

Different experimental studies[7−10] have been conducted on the reaction of nitrogen atoms with methyl radicals, to determine its kinetics and branching ratios. The reaction is found to be fast, with a rate coefficient of k=8.5×10^{-11} cm^3 s^{-1} molecule^{-1} at 298 K.[7] The observed branching ratios from discharge-flow techniques combined with mass spectrometry[9] are 0.9 for H_2-CN+H and 0.1 for the production of HCN. The experimental results are not easy to interpret in this case, as pointed out by Marston et al.,[9] because of the nature of the involved species. It is interesting to point out that the most obvious source of hydrogen cyanide is the $HCN + H_2$ channel. Nevertheless, it should be pointed out that this channel is in principle spin-forbidden. The ground-state reactants, $N(^4S) + CH_3(^2A''_2)$, should evolve initially on a triplet surface (the other possibility, a quintet surface, for the adiabatic evolution of the reactants lies clearly higher in energy).

A preliminary theoretical study of the $N(^4S) + CH_3$ reaction has been carried out by Gonzalez and Schlegel.[11] However, only a partial exploration of the potential surface was carried out in that study, and no attempt to evaluate the possible role of spin-forbidden paths was made. Nevertheless, their results support the $H_2CN + H$ channel as the dominant one. On the other hand, a theoretical study by Sadygov and Yarkony[12] focused on the spin-forbidden processes in the $N + CH_3$ reaction. In their work they did not explore exhaustively the potential surface, but they determined directly the minimum-energy crossing point (MECP) connecting the triplet and singlet surfaces. According to their calculations, the magnitude of the spin−orbit interaction (estimated to be about 30 cm^{-1}) and the local potential surface topology at the MECP suggest the viability of the intersystem crossing. Another recent theoretical work[13] on the title reaction has addressed the convergence of the energy differences on the triplet surface with respect to the size of the basis set and the nature of the correlation treatment.

In a series of recent papers,[14−19] we have provided computational studies of the reactions of ground-state and excited nitrogen atoms with halomethyl radicals (CH_2F, CH_2Cl, and CH_2Br). Quantitative estimations of the rate coefficients and branching ratios have been provided. In addition, the possible role of spin-forbidden processes has been considered. In all cases, even for those systems where spin−orbit interaction is noticeably high such as those containing chlorine or bromine, the reactions are predicted to take place with no change in the spin angular momentum. The high internal excitation of the MECP and the relative disposition of the involved species (the probability for intersystem crossing heavily depends not only on the magnitude of the spin−orbit interaction, but also on the velocity of the nuclei and on the gradients at the MECP) seem to be responsible for the marginal role of nonadiabatic channels in those reactions.

In the present work, a computational study of the reaction of ground-state nitrogen atoms with methyl radicals is reported.

* Corresponding autor. E-mail address: alargo@qf.uva.es.

10.1021/jp0634959 CCC: $33.50
Published on Web 08/26/2006

A complete exploration of both the triplet and singlet surfaces of the [NCH_3] system will be provided. On the basis of this exploration, a kinetic study within the frame of statistical theories will be carried out, as well as evaluation of the possible role of spin-forbidden processes for this reaction. In addition, a discussion of the reaction of excited nitrogen atoms, $N(^2D)$, with methyl radicals will be provided. Finally, a comparison with the analogous reactions with halomethyl radicals will be made when appropriate.

Computational methods

The optimizations of geometries and the vibrational frequency calculations were carried out at two different levels, namely second-order MØller−Plesset (MP2)[20] and density functional (DFT)[21] theories, employing Dunning's triple-ζ cc-pVTZ basis set.[22] We used the B3LYP model for the DFT calculations, which is a combination of Becke's 3-parameter exchange functional[23] and the correlation functional of Lee−Yang−Parr.[24] More accurate energies were obtained at both levels with the cc-pVXZ (X = D, T, Q) correlated-consistent basis set in order to estimate complete basis-set (CBS) limits. The CBS extrapolations are based on the property of correlation-consistent basis sets that exhibit monotonic convergence to an apparent complete basis set limit.[25] We used a mixed exponential/Gaussian function of the form

$$E(x) = E_{CBS} + B\exp[-(x-1)] + C\exp[-(x-1)^2] \quad (2)$$

where $x = 2$ (DZ), 3 (TZ), or 4 (QZ), and B and C are fitting constants.

To mitigate possible spin contamination effects on the convergence of the MP series, we employed approximate projected MP2 energies.[26] On the other hand, DFT calculations are virtually free of spin contamination. To further refine the electronic energy, we have also employed two different higher-levels of theory. G2[27] calculations were carried out, thus electronic energies are effectively computed (making additivity assumptions) at the QCISD(T)/6-311+G(3df,2p) level, where QCISD(T) stands for quadratic configuration interaction with single and double excitations followed by a perturbative treatment of triple excitations. The only difference with the standard G2 procedure was the use of projected-MP energies instead of unprojected ones. Finally, coupled cluster calculations,[28] CCSD(T)/cc-pVTZ, at the B3LYP geometries were carried out. This is a single- and double-excitation model augmented with a noniterative triple-excitation correction. The intrinsic reaction coordinate (IRC) method[29,30] was employed to verify that the transition states connect the desired minima on the potential energy surface (PES). The quantum chemical calculations were performed with the GAUSSIAN 98 package of programs.[31]

Kinetic calculations have been carried out within the framework of the statistical kinetic theories.[32] The formation of the initial intermediate and those processes where no transition structure was found (i.e., direct dissociations) were considered through the microcanonical variational transition state theory (μVTST) in its vibrator formulation.[33,34] Potential energy paths for those processes were first scanned. Subsequently, for each point of the scan, the Hessian matrixes, describing the modes orthogonal to the reaction path, were evaluated according to the procedure of Miller.[35,36]

For the unimolecular reactions involving all the intermediates, the microcanonical rate coefficients have been calculated employing the usual eq 3 of RRKM theory:[37]

$$k(E,J) = \sigma N^{\#}(E,J)/[h\rho(E,J)] \quad (3)$$

where, σ is the reaction symmetry factor and $N^{\#}(E,J)$ and $\rho(E,J)$ are, respectively, the number of states at the transition state and the density of states at the minimum evaluated for an energy E and a total angular momentum J.

The density and sum of states were determined employing the Forst algorithm[38] using the corresponding frequencies and moments of inertia. The possibility of tunneling was accounted for in terms of a monodimensional probability according to the generalized Eckart potential.[39] Finally, thermal rate coefficients were evaluated by averaging over the Boltzmann distribution. All the kinetic calculations were carried out employing the CCSD(T)/cc-pVTZ//B3LYP/cc-pVTZ energies and B3LYP/cc-pVTZ geometries and vibrational frequencies. Even though this approach based on statistical theories has well-known limitations,[32] in practice it is the only tool for study at a semiquatitative level of complicated reactions such as the present one.

We have searched for minimum-energy crossing points (MECPs), that is, the minimum of the hyperline of intersection[40−45] between the singlet and triplet surfaces. The MECP is obtained through a hybrid method which employs accurate geometrical optimization[46−48] at the B3LYP level, followed by a refinement at the CCSD(T)/cc-pVTZ//B3LYP/cc-pVTZ level. An estimation of the curvature of the seam,[48,50] and therefore an approximate determination of the zero-point vibrational energy (ZPVE) at the MECPs, has also been carried out. The elements of the approximate mono-electronic[51] spin−orbit coupling Hamiltonian matrix, providing an estimation of the magnitude of the coupling between the two surfaces, have been calculated for the MECPs structures using first-order configuration interaction (FOCI) wave functions constructed using the natural orbitals from a state averaged CASSCF calculation. To ascertain the actual role played by the located MECPs, i.e., which minima are actually interconnected through MECPs, a rough IRC-like procedure has been applied.

The spin-forbidden processes have been accounted for by means of a nonadiabatic version of the RRKM theory.[41,50] In such cases the unimolecular rate coefficients are computed as

$$k(E,J) = \frac{2}{h\rho(E,J)}\int_0^E \rho^{MECP}(E-E_h,J)P(E_h,J)\,dE_h \quad (4)$$

where E_h is the fraction of the nonfixed energy reversed in the coordinate orthogonal to the seam, and $\rho^{MECP}(E-E_h,J)$ is the density of the states at the minimum energy crossing point (MECP). In the above formula $P(E_h,J)$ represents the surface hopping probability, which has been evaluated by the monodimensional Delos model.[52,53]

Results and Discussion

[NCH_3] Triplet PES. The relative energies of the possible products and relevant minima and transition states on the triplet PES for the $N(^4S) + CH_3(^2A''_2)$ reaction are given in Table 1. In addition, the energetic profile for the reaction at selected levels of theory (CCSD(T) and G2) is shown in Figure 1. The geometrical parameters for all involved species are provided as Supporting Information (Figures S1−S3). We have checked that intermediates, as well as reactants and products, correspond to local minima with all real vibrational frequencies, whereas transition structures exhibit one imaginary frequency corresponding to the desired normal mode.

The B3LYP and MP2 geometrical parameters collected in Figures S1−S3 show a reasonable agreement between both levels of theory. There is only one discrepancy between both

TABLE 1: Relative Energies (in kcal/mol) at Different Levels of Theory for the Different Species Involved in the Reaction of N(^{4}S) with CH_3 on the Triplet PES

system	PMP2/CBS[a]	B3LYP/CBS[b]	CCSD(T)/cc-pVTZ[b]	G2
$CH_3(^2A_2")$ + N(^{4}S)	0.0	0.0	0.0	0.0
trans-HC=NH + H	−34.6	−34.9	−23.3	−26.2
cis-HC=NH + H	−30.2	−31.0	−18.9	−21.6
H_2CN + H	−39.3	−42.8	−32.2	−34.8
H_2NC + H	−11.5	−12.6	−1.8	−10.2
HCN(^{3}A) + $H_2(^1\Sigma_g)$	0.6	−11.4	−1.7	−9.9
HNC(^{3}A) + $H_2(^1\Sigma_g)$	8.3	0.5	10.4	2.0
^{3}I1	−70.1	−76.4	−65.7	−73.2
^{3}I2	−58.4	−66.5	−51.8	−60.1
^{3}I3	−58.5	−60.9	−48.1	−56.5
TS1	−35.1	−41.1	−29.2	−37.5
TS2	−27.9	−33.9	−21.2	−29.1
TS3	−19.5	−23.0	−9.6	−18.0
TS4	−26.6	−31.5	−18.0	−27.8
TS5	−31.9	−39.2	−25.7	−34.0
TS6	−22.2	−29.0	−14.6	−22.9
TS7	−10.5	−−−	−−−	−10.6

[a] Including ZPVE at the MP2/cc-pVTZ level. [b] Including ZPVE at the B3LYP/cc-pVTZ level.

levels. At the MP2 level we were able to locate a transition state (TS7) for the hydrogen atom elimination from I3 to give H_2NC, whereas at the B3LYP level this is a direct process. Nevertheless, at the G2 level TS7 is found slightly below the products, showing that at higher levels of theory this should be a direct process without any barrier other than its endothermicity.

Concerning the performance of the different levels of theory, inspection of Table 1 shows that the MP2/CBS relative energies are rather close to the G2 ones, suggesting that refinement of the energy at the G2 level has only a minor effect. On the other hand, B3LYP and CCSD(T) relative energies are quite different. In this case it seems that B3LYP energies might be not accurate enough, especially for the computation of energy barriers. It is also interesting to notice that CCSD(T)/ cc-pVTZ relative energies are systematically above the G2 ones (in most cases by 3−8 kcal/mol). In our previous studies on the $CH_2X(^2A')$ + N(^{4}S) reactions,[14,16,18] we observed a similar behavior. We concluded that the discrepancy between the CCSD(T) and G2 energies is related, at least in part, to the description of N(^{4}S), since the G2 method includes a higher-level empirical correction (HLC) which seems to be important for the description of N(^{4}S). The fact that if the relative energies are computed with respect to one of the intermediates the CCSD(T) values get closer to the G2 ones seems to point in that direction. A second source of discrepancy could be spin contamination, but this is not severe in most cases.

The approach of reactants proceeds through an attractive potential surface leading to intermediate ^{3}I1, H_3CN, whose formation is then a direct process which does not involve any barrier. This is not surprising, since radical−radical reactions generally proceed on potential energy surfaces that have no maximum.[54] ^{3}I1 is in fact the most stable stationary point on the triplet surface. Once ^{3}I1 is formed, we have basically two different possibilities for its further evolution. In the first place, elimination of a hydrogen atom would lead to H_2CN+H, the most exothermic channel. This process involves a transition state, **TS1**, which lies well below the reactants. A second possibility is isomerization into ^{3}**I2**, H_2CNH, through hydrogen migration from carbon to nitrogen, which proceeds through **TS2**. **TS2**, even though it lies also below the reactants, is clearly located higher in energy than **TS1**. ^{3}**I2** may lead to both H_2CN + H and t-HCNH + H, the former one involving a lower barrier. Isomerization of ^{3}I2 into ^{3}I3, $HCNH_2$, involves even a higher barrier, and is required to produce the H_2NC + H channel as

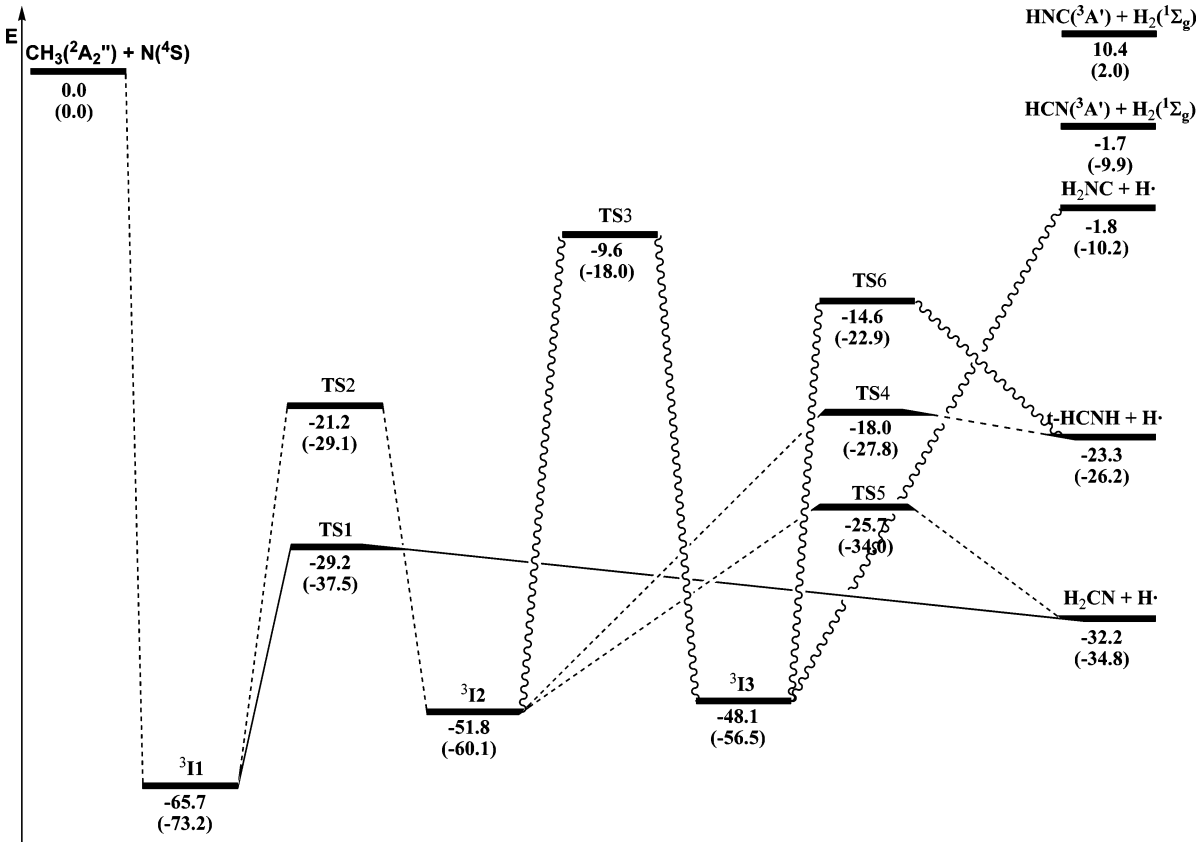

Figure 1. Reaction profile (kcal/mol) at the CCSD(T)/cc-pVTZ and G2 (in parentheses) levels for the reaction N(^{4}S) + CH_3 on the triplet PES.

SCHEME 1: Mechanistic Model for the Kinetic Study Employed in the Present Work[a]

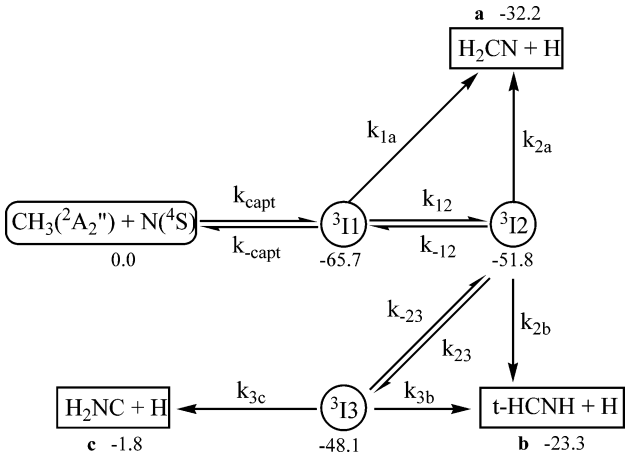

[a] Relative energies at 0 K are in kcal/mol and were computed at the CCSD(T)/cc-pVTZ level, including B3LYP/cc-pVTZ ZPVEs.

final product. We have also included in Figure 1 the HCN(^{3}A′) + H_2 and HNC(^{3}A′) + H_2 channels. Only the former one is slightly exothermic. We have not been able to locate transition states for the formation of either HCN or HNC on the triplet surface. However, they should not compete with the rest of channels because the barrier for their production should be in any case higher given their relative stability.

The overall features of the triplet PES for the N(^{4}S) + CH_3 reaction are rather similar to those of the analogous reactions of ground-state nitrogen atoms with halomethyl radicals, N(^{4}S) + CH_2X (X being F, Cl, or Br).[14,16,18] In all cases the initial intermediate ^{3}I1, which is formed in a direct process without any barrier, is the most stable stationary point on the triplet PES and is located 60−70 kcal/mol below the reactants. The main difference concerns the nature of the most exothermic product. For CH_3, CH_2Cl, and CH_2Br as reactants, the most exothermic channel leads to H_2CN (through elimination of H, Cl, and Br, respectively). On the other hand, in the case of CH_2F, the most exothermic channel involves elimination of a hydrogen atom leading to HFCN. Quite likely the stronger C−F bond, when compared with the C−Cl or C−Br bonds, is largely responsible for the different behavior of halomethyl radicals.

Kinetic Calculations. On the basis of the triplet PES for the [NCH_3] system, we have developed a mechanistic model for the reaction of ground-state nitrogen atoms with methyl radicals. The mechanistic model is depicted in Scheme 1. As can be seen we have included the three most exothermic channels, that is, H_2CN + H (channel a), t-HCNH + H (channel b), and H_2NC + H (channel c). Those channels leading to either HCN or HNC in a triplet state should be even less important than channel c.

According to the mechanistic model shown in Scheme 1, the steady-state solution of the kinetic equations derived from the mechanistic model shown in Scheme 1 leads to

$$k_{\text{overall}} = k_a + k_b + k_c \tag{5}$$

where the individual coefficients are given by the following expressions:

$$k_a = \frac{k_{\text{capt}}}{A}\left\{k_{1a} + \frac{k_{12}k_{2a}}{k_{-12} + k_{2a} + k_{2b}}\right\} \tag{6}$$

$$k_b = \frac{k_{\text{capt}}k_{12}}{A(k_{-12} + k_{2a} + k_{2b})}\left\{k_{2b} + \frac{k_{23}k_{3b}}{k_{-23} + k_{3b} + k_{3c}}\right\} \tag{7}$$

$$k_c = \frac{k_{\text{capt}}k_{12}k_{23}k_{3c}}{A(k_{-12} + k_{2a} + k_{2b})(k_{-23} + k_{3b} + k_{3c})} \tag{8}$$

where

$$A = k_{-\text{capt}} + k_{12} + k_{1a} - \frac{k_{12}k_{-12}}{k_{-12} + k_{2a} + k_{2b}} \tag{9}$$

The final canonical coefficients have been obtained after thermal average according to a Boltzmann distribution.

The overall and individual rate coefficients are represented in Figure 2 as functions of the temperature. It is readily seen in Figure 2 that the individual rate coefficient for channels b and c are so small that they practically superpose with the abscissa. Consequently, the rate coefficient for channel a virtually coincides with the overall rate coefficient. The first conclusion is obviously that the dominant channel should be the production of H_2CN + H, which is therefore not only thermodynamically but also kinetically favored. This is clearly illustrated by the product branching ratios given in Table 2, where it can be seen that at any temperature the branching fraction for H_2CN is 0.997. Only residual quantities of t-HCNH (always below 0.0027) are formed, whereas for H_2NC the branching fraction is negligible.

The results from the kinetic calculation are consistent with the general overview of the triplet PES for the N(^{4}S) + CH_3 reaction. The dominant channel, H_2CN + H, proceeds through **TS1**, which is the lowest-lying transition state on the triplet PES. Channels b and c necessarily imply at least isomerization of ^{3}I1 into ^{3}I2, which involves a transition state, **TS2**, lying higher (about 8 kcal/mol) in energy than **TS1**. Furthermore, once ^{3}I2 is formed, the path involving the lowest-lying transition state is also that leading to H_2CN + H, since **TS5** lies lower in energy than **TS3** and **TS4**. The kinetic calculations are then in complete agreement with the essential features of the triplet PES. They also agree with the experimental observation that the dominant product is H_2CN.[9]

The computed rate coefficient for the overall process at 298 K is 9.1×10^{-12} cm^3 s^{-1} molecule^{-1}. This value is considerably higher than the rate coefficients obtained for the reactions of ground-state nitrogen atoms with halomethyl radicals,[15,16,18]

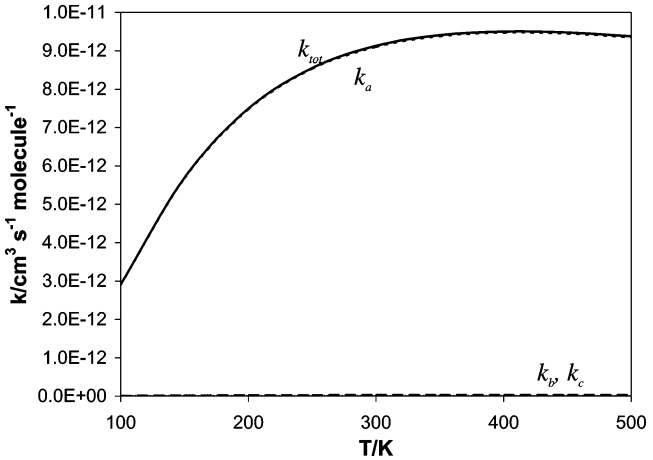

Figure 2. Overall and individual canonical rate coefficients (cm^{-3} s^{-1} molecule^{-1}) plotted vs temperature.

TABLE 2: Reaction Product Branching Fractions at Different Temperatures

T/K	$H_2CN + H$	*t*-HCNH + H	$H_2NC + H$
100	0.99750	0.00250	0.00001
150	0.99748	0.00251	0.00001
200	0.99747	0.00252	0.00001
250	0.99744	0.00255	0.00001
300	0.99741	0.00257	0.00001
350	0.99738	0.00261	0.00001
400	0.99734	0.00265	0.00001
450	0.99730	0.00269	0.00001
500	0.99725	0.00274	0.00001

which are in the range $3-13 \times 10^{-13}$ cm^3 s^{-1} molecule^{-1}. However, this value is 1 order of magnitude lower than the experimental[7] result for the N(^{4}S) + CH_3 reaction, k=8.5 $\times$ 10^{-11} cm^3 s^{-1} molecule^{-1}. Employing the B3LYP energy values a somewhat smaller value is obtained (7.6 $\times$ 10^{-12} cm^3 s^{-1} molecule^{-1}), although essentially of the same order of magnitude than at the CCSD(T) level. Nevertheless, it is significant that employing the same model and levels of theory the estimated rate coefficient for the present reaction is higher than those found for similar reactions of ground-state nitrogen atoms with halomethyl radicals. The main conclusion should be that the process is fast and efficient, and certainly considerably faster than the analogous reactions with halomethyl radicals. Therefore, the main discrepancy with the experimental results is not the magnitude of the rate coefficient, but the small fraction (about 10%) of HCN observed in the experiments.[9]

Marston et al.[9] and Sadygov and Yarkony[12] have suggested that the spin-forbidden channel HCN($^1\Sigma^+$) + H_2($^1\Sigma g^+$) could account for the observed hydrogen cyanide. On the other hand, Gonzalez and Schlegel[11] have suggested that secondary processes, such as N(^{4}S) + $H_2CN \rightarrow$ HCN($^1\Sigma^+$) + NH, could contribute to the disappearance of H_2CN and production of hydrogen cyanide. To ascertain the possible role of spin-forbidden processes in the N(^{4}S) + CH_3 reaction, we have accomplished a detailed computational study. The first step is to explore the singlet PES of the [NCH_3] system.

Singlet PES. We have searched for relevant minima and transition states connecting them on the singlet [NCH_3] PES. The corresponding geometrical parameters for the minima are provided in Figure S4, whereas those of the transition states are given in Figure S5. The geometries of the possible products are also shown in Figure S1. The energies, relative to N(^{4}S) + CH_3($^2A''_2$), of the possible products and relevant minima and transition states on the singlet PES are given in Table 3. Since these data might also be useful to obtain some conclusions about the reaction of excited nitrogen atoms with methyl radical, an energy profile for that reaction, N(^{2}D) + CH_3($^2A''_2$), is depicted in Figure 3. In that case the energies of all species have been computed relative to those reactants. Incidentally, one can note that the G2 and CCSD(T) levels provide quite close similar results when the energies are taken relative to N(^{2}D) + CH_3. On the other hand, similar differences as those observed for the triplet species are found when the energies are computed taking as reference ground-state nitrogen atoms. This observation supports our previous conclusion attributing to the difference in describing N(^{4}S) the major source of discrepancy between both levels of theory.

^{1}I1 is the only intermediate on the singlet surface which is less stable than its triplet counterpart. Nevertheless, the energy difference between ^{1}I1 and ^{3}I1 is relatively small. This is probably due to their similar electronic structure. In fact, both species differ only in two unpaired electrons located at nitrogen in ^{3}I1 which are paired in the singlet species. In this case such similarity produces not only similar geometrical parameters, but

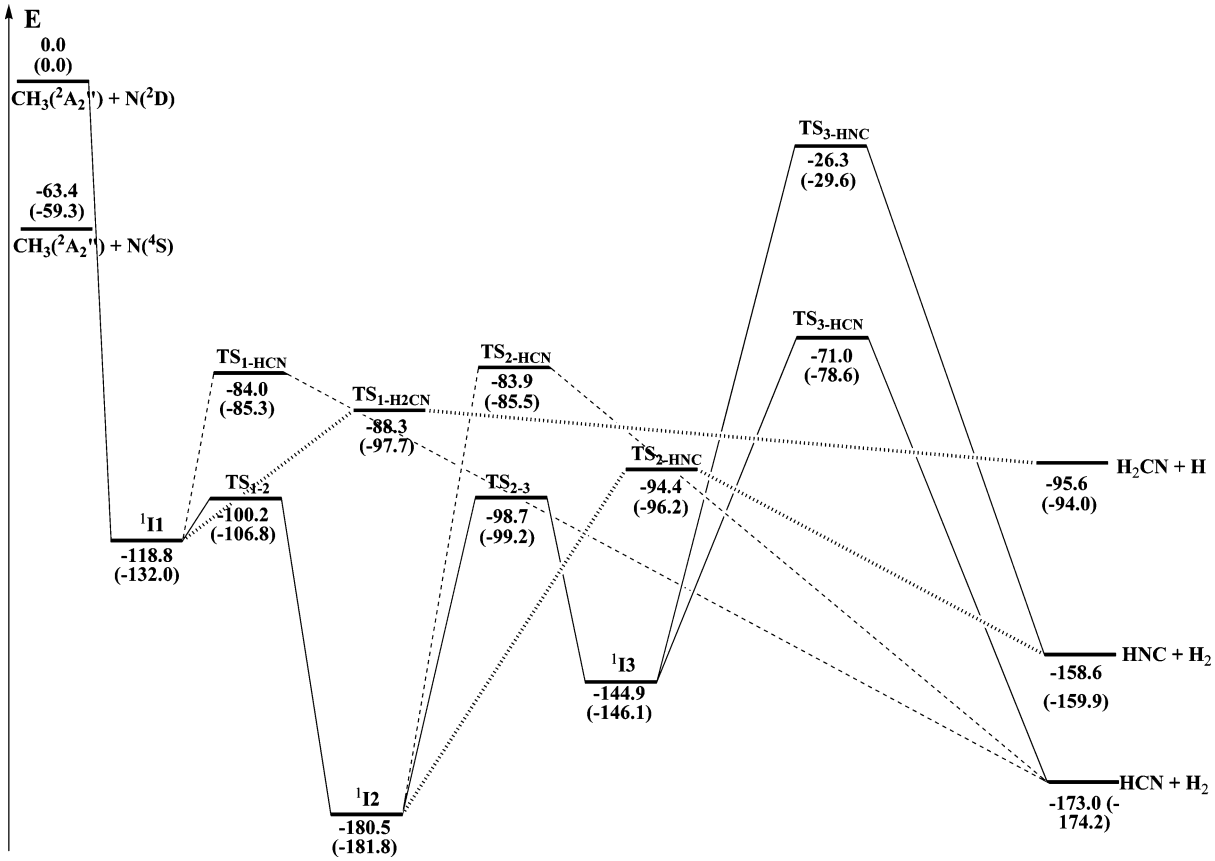

Figure 3. Reaction profile (kcal/mol) at the CCSD(T)/cc-pVTZ and G2 (in parentheses) levels for the reaction N(^{2}D) + CH_3 on the singlet PES.

TABLE 3: Relative Energies (in kcal/mol) at Different Levels of Theory for the Different Species Involved in the Reaction of N(^{2}D) with CH_3 on the Singlet PES

system	PMP2/CBS[a]	B3LYP/CBS[b]	CCSD(T)/cc-pVTZ[b]	G2
$CH_3(^2A_2")$ + N(^{4}S)	0.0	0.0	0.0	0.0
$CH_3(^2A_2")$ + N(^{2}D)	72.9	63.0	63.4	59.3
H_2CN + H	−39.3	−42.8	−32.2	−34.7
HCN + H_2	−123.9	−117.0	−109.6	−114.9
HNC + H_2	−106.3	−103.4	−95.2	−100.6
^{1}I1	−68.6	−65.6	−55.4	−72.7
^{1}I2	−129.0	−126.7	−117.1	−122.5
^{1}I3	−91.0	−92.2	−81.5	−86.8
TS_{1-2}	−37.6	−49.9	−36.8	−47.5
TS_{1-HCN}	−26.2	−34.7	−20.6	−26.0
TS_{1-H2CN}	−21.8	−37.7	−24.9	−38.4
TS_{2-3}	−47.1	−46.1	−35.3	−39.9
TS_{2-HCN}	−33.1	−32.1	−20.5	−26.2
TS_{2-HNC}	−40.6	−43.3	−31.0	−36.9
TS_{3-HCN}	−12.3	−19.3	−7.6	−19.3
TS_{3-HNC}	30.9	27.1	37.1	29.7

[a] Including ZPVE at the MP2/cc-pVTZ level. [b] Including ZPVE at the B3LYP/cc-pVTZ level.

also a close relative energy. The rest of intermediates, ^{1}I2 and ^{1}I3, are considerably more stable than the corresponding triplets. The stability of the ^{1}I2 and ^{1}I3 species, as well as the much shorter C−N distances observed for the singlet than for the triplet intermediates, reflect the formation of much stronger C−N bonds between carbon and nitrogen atoms in the case of singlet species. The planarity of the singlet H_2CNH (^{1}I2) and $HCNH_2$ (^{1}I3) intermediates is also related to strong C−N bonds.

The possible evolution of the intermediates on the singlet surface can be seen in Figure 3. We have only represented the three most exothermic channels, namely, formation of singlet HCN or HNC (through elimination in both cases of a hydrogen molecule), and the lowest-lying channel involving elimination of a hydrogen atom leading to H_2CN + H. The latter is the most favored channel observed on the triplet surface. As expected, the HCN + H_2 and HNC + H_2 channels are much more exothermic than any of the channels observed on the triplet surface. Obviously, production of hydrogen cyanide is thermodynamically favored. However, formation of HCN from both ^{1}I1 and ^{1}I2 seems to involve higher energy barriers than other competitive processes. TS_{1-HCN}, the transition state associated to the formation of HCN + H_2 from ^{1}I1, lies higher in energy than the transition states for isomerization into ^{1}I2 and for H_2CN production. The same occurs for TS_{2-HCN}, the transition state involved in the formation of HCN from ^{1}I2, since it lies higher in energy than both TS_{2-3} and TS_{2-HNC}. The only case where formation of HCN has a lower barrier than production of HNC is ^{1}I3. However, in that case the involved transition states for both HCN and HNC formation lie higher in energy than the rest of transition states. Therefore, it seems that probably HCN should not be the most favored channel from the kinetic point of view. Furthermore, we should point out that all transition states leading to the HCN + H_2 channel on the singlet PES lie higher in energy (at least 9 kcal/mol) than the transition state TS1 on the triplet PES involved in the production of H_2CN + H from ^{3}I1. A kinetic computational study for the reaction N(^{2}D) + $CH_3(^2A")_2$) could be in principle questioned given the relatively high internal energies of the intermediates on the singlet PES,[17] especially ^{1}I2 and ^{1}I3. However, we have computed the rate coefficients for the different processes depicted in Figure 3 in terms of the statistical kinetic theories. We have obtained in all cases values which are compatible with the possibility of randomization of the internal energy. The relatively high barriers for the evolution of energized intermediates (see Figure 3) could be a key factor for such behavior. A similar kinetic treatment to that outlined above for the N(^{4}S) + CH_3 on the triplet PES produces the following branching ratios at 298 K for the N(^{2}D) + CH_3 reaction: 0.745 for H_2CN + H; 0.184 for HCN + H_2; and 0.071 for HNC + H_2. Modification of the temperature in the range 100−500 K alters these branching ratios only in the third decimal figure. Therefore, it seems that on the singlet PES the preferred product from the kinetic point of view is again H_2CN + H, that is, the most favored channel on the triplet PES. Nevertheless, the production of HCN is significant and even formation of HNC is nonnegligible.

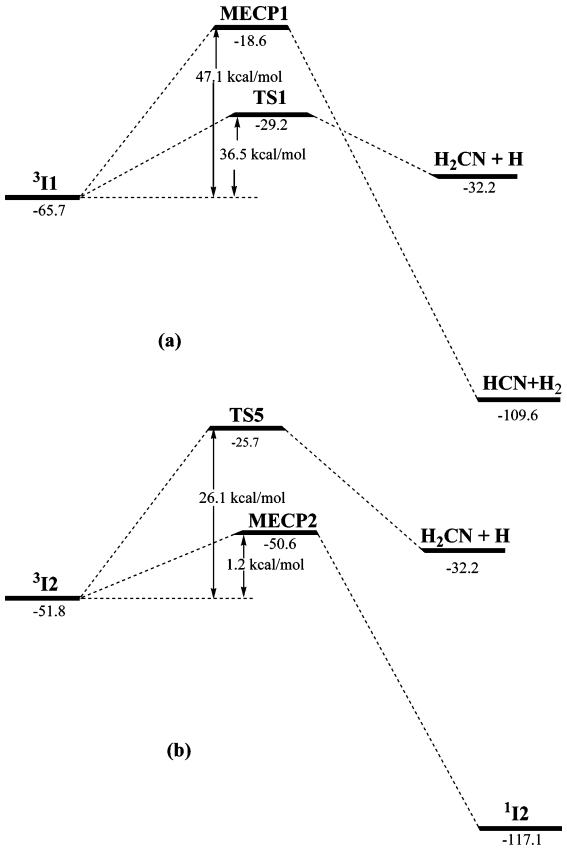

Figure 4. Potential energy schemes (kcal/mol) comparing the relative energies at the CCSD(T) level of the different MECPs of the N(^{4}S) + CH_3 reaction with the corresponding competing adiabatic processes.

Spin-Forbidden Processes. In any case the crucial question remains the accessibility of the singlet PES from the N(^{4}S) + $CH_3(^2A"_2)$ reactants. We have characterized two different MECPs connecting the triplet and singlet surfaces, whose geometrical parameters are given in Figure S6. One of them, denoted as MECP1, connects ^{3}I1 directly with the products H_2CN + H, according to the IRC calculation. The second one, MECP2, corresponds to the transition between ^{3}I2 and ^{1}I2, the H_2CNH species on both surfaces. The corresponding values for the spin−orbit coupling are relatively low, namely, 23.0 cm^{-1} (MECP1) and 10.5 cm^{-1} (MECP2). MECP1 has geometrical parameters close to the MECP characterized by Sadygov and Yarkony.[12] These authors also estimated the spin−orbit interaction in the vicinity of the MECP to be 30 cm^{-1}. Sadygov and Yarkony[12] observed the incipient formation of a H−H bond in the MECP, suggesting that in fact this MECP connects ^{3}I1 directly with H_2CN + H. In Figure 4 we show potential energy-schemes for the spin-forbidden processes and their main competing adiabatic paths, that is formation of H_2CN + H from

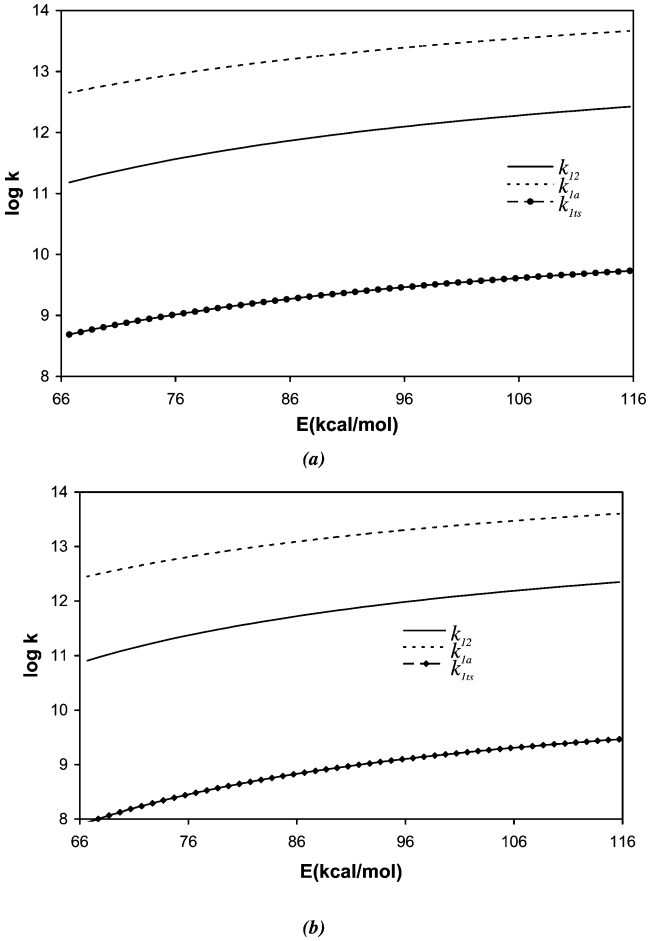

Figure 5. $J = 0$ (a) and 40 (b) microcanonical rate coefficients (s^{-1}) for the nonadiabatic process (k_{1ts}) involving MECP1 as functions of the internal energy, compared with its competing adiabatic processes. See Scheme 1 for the definition of coefficients.

^{3}I1 and ^{3}I2. Sadygov and Yarkony[12] suggested that the spin-crossing through MECP1 could proceed with a significant probability as to account for the HCN production in the N(^{4}S) + CH_3 reaction. However, it is clearly seen in Figure 4 that the barrier for the spin crossing from ^{3}I1 is more than 10 kcal/mol higher than the barrier for production of H_2CN on the triplet PES. On the other hand, MECP2 lies well below TS5, the transition state for H_2CN formation from ^{3}I2. In fact MECP2 is located only 1.2 kcal/mol higher in energy than ^{3}I2.

To definitively ascertain the role of spin crossing in the N(^{4}S) + CH_3 reaction, we have calculated the microcanonical rate coefficients of the nonadiabatic processes, ^{3}I1→ ^{1}I1 (k_{1ts}) and ^{3}I2→ ^{1}I2 (k_{2ts}). Their values, at different internal energies and two particular values of angular momenta ($J = 0$ and $J = 40$), are shown in Figures 5 and 6, respectively, compared with the coefficients for the main competing processes on the triplet surface. In Figure 5 k_{12} and k_{1a} refer to the ^{3}I1→ ^{3}I2 and ^{3}I1→ H_2CN + H processes, respectively. In Figure 6 k_{23}, k_{2a}, and k_{2b} correspond to the ^{3}I2→ ^{3}I3, ^{3}I2→ H_2CN + H, and ^{3}I2→ t-HCNH + H processes, respectively. Our results suggest that, at any value of internal energy and angular momentum, the rate coefficients of the nonadiabatic processes are of scarce relevance when compared to the spin-conserving channels. This result seems to be due to the simultaneous occurrence of low spin−orbit coupling, high internal excitation of the MECPs, and the relative disposition of the involved species, since the probability for intersystem crossing depends on the velocity of the nuclei and on the gradients at the MECP. In addition, in the case of MECP1 another factor is its relatively high energy respect to the triplet intermediate.

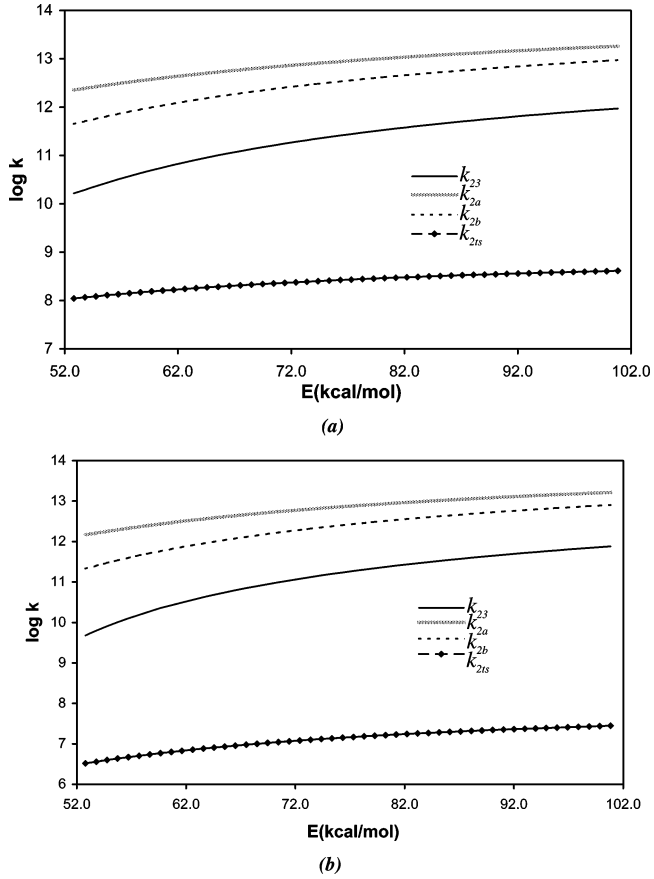

Figure 6. $J = 0$ (a) and 40 (b) microcanonical rate coefficients (s^{-1}) for the nonadiabatic process (k_{2ts}) involving MECP2 as functions of the internal energy, compared with its competing adiabatic processes. See Scheme 1 for the definition of coefficients.

The results shown in Figures 5 and 6 suggest that the reaction N(^{4}S) + CH_3 is likely to proceed without any change in the spin angular momentum. To further confirm this conclusion, we have incorporated into the mechanistic model for the N(^{4}S) + CH_3 reaction (shown in Scheme 1) the spin-forbidden process leading directly to H_2CN + H. In fact this is the only reasonable spin-forbidden process that could be competitive, since it has been shown in the previous kinetic analysis of the triplet PES that the following path:

$$N(^4S) + CH_3 \rightarrow {}^3H_3CN \rightarrow TS1 \rightarrow H_2CN + H \quad (10)$$

is the dominant one, mainly because TS1 lies much below TS2, the transition state for ^3H_3CN → ^3H_2CNH isomerization. Therefore the role of ^{3}I2, the intermediate from which the second spin-forbidden process (involving MECP2) should start, is rather limited.

The result of such kinetic study, including spin-crossing, leads to a final result for the branching ratios virtually coincident with the previously shown in Table 2. The branching fraction for HCN + H_2 accounts to namely 3×10^{-5}. It seems clear according to our calculations that spin-forbidden processes are highly unlikely for the present reaction, and do not seem to explain the observed 10% of HCN + H_2 in the experiments.[9]

The question now is how to explain this contradiction, assuming of course that the experimental results are correctly interpreted. A clue is already given in the original paper by Gonzalez and Schlegel[11] and also pointed out by Hadjebar et

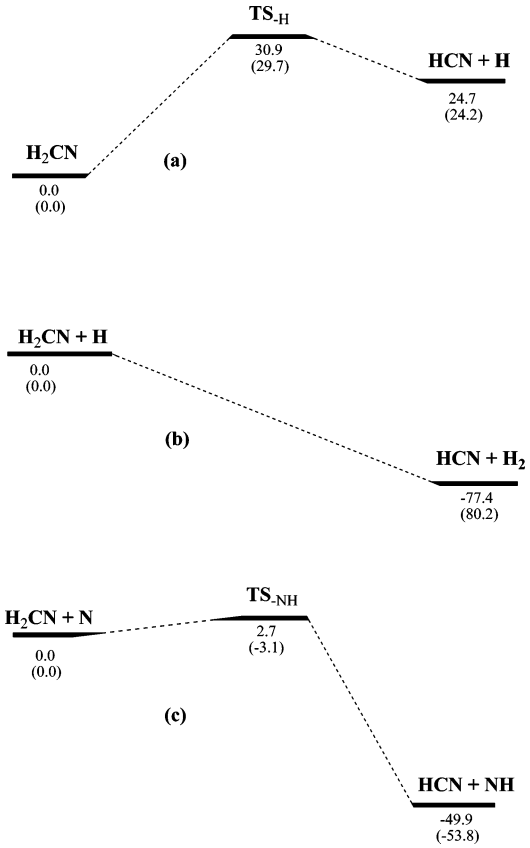

Figure 7. Potential energy schemes (kcal/mol) at the CCSD(T) and G2 (in parentheses) levels for the possible further evolution of H_2CN.

al..[13] These authors did not attempt any investigation of the possible role of spin-forbidden processes, but suggested that further evolution of the preferred products, $H_2CN + H$, might finally lead to the formation of hydrogen cyanide. In both papers the authors point to the unimolecular decomposition of H_2CN, through the elimination of a hydrogen atom, as a possible source of HCN. In addition, Gonzalez and Schlegel[11] suggested that H_2CN can also participate in bimolecular reactions, such as recombination with hydrogen atoms or abstraction of a hydrogen atom by ^4N. Therefore, we have taken into account the following possibilities:

$$H_2CN \rightarrow HCN + H \quad (11)$$

$$H_2CN + H \rightarrow HCN + H_2 \quad (12)$$

$$H_2CN + N(^4S) \rightarrow HCN + {}^3NH \quad (13)$$

Potential energy schemes for these processes are represented in Figure 7. It is clearly seen that process (11) is not favorable, since it implies a noticeable barrier (even though the corresponding TS still lies slightly below the initial reactants, $N(^4S) + CH_3$). On the other hand, recombination of H_2CN with hydrogen atoms leading to elimination of a hydrogen molecule does not seem to be subject to any barrier. We have search for a possible transition state associated to this process. Actually, we were able to locate a transition state (at the unrestricted level on the singlet surface), but it was found to lie below $H_2CN + H$ (−1.5 and −14.2 kcal/mol, respectively, at the CCSD(T) and G2 levels). Therefore, this seems to be a direct process which does not involve any barrier. Finally, for the reaction of H_2CN with nitrogen atoms, process (13), we found a transition state lying just 2.7 kcal/mol higher in energy (−3.1 kcal/mol at the G2 level). Consequently, this process must be subject to a very small barrier. Furthermore, the corresponding transition state lies well below the initial reactants $N(^4S) + CH_3$.

The main conclusion from these studies is that further evolution of the preferred products in the reaction of ground-state nitrogen atoms with methyl radicals, $H_2CN + H$, might finally lead to the formation of hydrogen cyanide. This could explain the fraction of HCN observed in the experiments.

Conclusions

A computational study of the reaction of ground-state nitrogen atom with the methyl radical has been carried out. The reactants approach through an attractive potential surface leading to an intermediate $^3I1$, H_3CN, whose formation is barrier-free.

In agreement with the experimental results, as well as with previous theoretical studies, the dominant channel for this reaction is $H_2CN + H$, with branching ratios around 0.997. Only residual quantities of t-HCNH (with branching ratios below 0.003 at any temperature) are formed, whereas for H_2NC the branching fraction is negligible. The analysis of the PES shows that the preferred reaction path is elimination of a hydrogen atom from the initially formed intermediate, triplet H_3CN.

A kinetic computational study provides a rate coefficient for the overall process at 298 K of 9.1×10^{-12} cm^3 s^{-1} molecule^{-1}, which is nearly 1 order of magnitude lower than the experimental[7] result for the $N(^4S) + CH_3$ reaction, namely, $k = 8.5 \times 10^{-11}$ cm^3 s^{-1} molecule^{-1}. However the theoretically estimated rate coefficient is much larger than those computed for the reactions of ground-state nitrogen atoms with halomethyl radicals[15,16,18], which are in the range $3-13 \times 10^{-13}$ cm^3 s^{-1} molecule^{-1}.

The analysis of the singlet PES, and the corresponding computational kinetic study, shows that for the reaction of excited nitrogen atoms with methyl radicals the preferred product from the kinetic point of view is again $H_2CN + H$. Nevertheless, in this case the production of HCN is significant (with branching ratios around 0.185), and even formation of HNC is nonnegligible.

We have considered the possibility of spin-crossing from the triplet to the singlet PES. According to our calculations, spin-forbidden processes are highly unlikely for the present reaction, and the reaction of ground-state nitrogen atoms with methyl radicals should proceed without any change in the spin angular momentum. Nevertheless, we have shown that further evolution of the preferred products, $H_2CN + H$, might finally lead to the formation of hydrogen cyanide and consequently could explain the small amount of hydrogen cyanide observed in the experiments.[9]

Acknowledgment. This research has been supported by the Ministerio de Educación y Ciencia of Spain (Grants CTQ2004-07405-02-01) and by the Junta de Castilla y León (Grant VA085/ 03). The authors gratefully acknowledge Prof. José A. Sordo (Universidad de Oviedo) and Prof. Massimiliano Aschi (Universitá di L′Aquila) for very helpful comments.

Supporting Information Available: Geometries of the different species studied in the present work (Tables S1−S6). Full version of ref 31. This material is available free of charge at http://pubs.acs.org.

References and Notes

(1) Yung, Y. L.; Allen, M.; Pinto, J. P. *Astrophys. J. Suppl. Ser. Phys* **1984**, *55*, 465.

(2) Lellouch, E.; Romani, P. N.; Rosenqvist, J. *Icarus* **1994**, *108*, 112.

(3) Wayne, R. P. *Chemistry of Atmospheres*; Oxford University Press: Oxford, 1991.
(4) Nejad, L. A. M.; Millar, T. J. *Mon. Not. R. Astron. Soc.* **1988**, *230*, 79.
(5) Glarborg, P.; Miller, J. A.; Kee, R. J. *Combust. Flame* **1986**, *65*, 177.
(6) Safrany, D. R. *Prog. React. Kinet.* **1971**, *6*, 1.
(7) Stief, L. J.; Marston, F. L.; Nava, D. F.; Payne, W. A.; Nesbitt, F. L. *Chem. Phys. Lett.* **1988**, *147*, 570.
(8) Marston, G.; Nesbitt, F. L.; Nava, D. F.; Payne, W. A.; Stief, L. J. *J. Phys. Chem.* **1989**, *93*, 5769.
(9) Marston, G.; Nesbitt, F. L.; Stief, L. J. *J. Chem. Phys.* **1989**, *91*, 3483.
(10) Stief, L. J.; Nesbitt, F. L.; Payne, W. A. *J. Chem. Phys.* **1995**, *102*, 5309.
(11) Gonzalez, C.; Schlegel, H. B. *J. Am. Chem. Soc.* **1992**, *114*, 9118.
(12) Sadygov, R. G.; Yarkony, D. R. *J. Chem. Phys.* **1997**, *107*, 4994.
(13) Hadjebar, I.; Achour, M. N.; Boucekkine, A.; Berthier, G. *Chem. Phys.* **2001**, *264*, 153.
(14) Menendez, B.; Rayon, V. M.; Sordo, J. A.; Cimas, A.; Barrientos, C.; Largo, A. *J. Phys. Chem. A* **2001**, *105*, 9917.
(15) Cimas, A.; Aschi, M.; Barrientos, C.; Rayon, V. M.; Sordo, J. A.; Largo, A. *Chem. Phys. Lett.* **2003**, *374*, 594.
(16) Cimas, A.; Rayon, V. M.; Aschi, M.; Barrientos, C.; Sordo, J. A.; Largo, A. *J. Phys. Chem. A* **2005**, *109*, 6540.
(17) Cimas, A.; Rayon, V. M.; Aschi, M.; Barrientos, C.; Sordo, J. A.; Largo, A. *J. Chem. Phys.* **2005**, *123*, 114312.
(18) Cimas, A.; Rayon, V. M.; Aschi, M.; Barrientos, C.; Sordo, J. A.; Largo, A. *Int. J. Mass Spectrom.*. **2006**, *249*, 451.
(19) Cimas, A.; Rayon, V. M.; Barrientos, C.; Aschi, M.; Sordo, J. A.; Largo, A. *Chem. Phys. Lett.* **2006**, *422*, 276.
(20) Hehre, W. J.; Radom, L.; Schleyer, P.v. R.; Pople, J. A. *Ab initio Molecular Orbital Theory*; Wiley: New York, 1986.
(21) Koch, W.; Holthausen, M. C. *A Chemist*'s *Guide to Density Functional Theory*, 2nd ed.; Wiley-VCH: Weinheim, Germany, 2000.
(22) Dunning, T. H., Jr. *J. Chem. Phys.* **1989**, *90*, 1007.
(23) Becke, A. D. *J. Chem. Phys.* **1992**, *97*, 9173.
(24) Lee, C.; Yang, W.; Parr, R. G. *Phys. Rev. B* **1988**, *37*, 785.
(25) Dunning, T. H., Jr. *J. Phys. Chem. A* **2000**, *104*, 9062.
(26) Schlegel, H. B. *J. Chem. Phys.* **1986**, *84*, 4530.
(27) Curtiss, L. A.; Raghavachari, K.; Trucks, G. W.; Pople, J. A. *J. Chem. Phys.* **1991**, *94*, 7221.
(28) Bartlett, R. J., Stanton, J. F., *Reviews in Computational Chemistry*; VCH: New York, 1994; Vol. 5.
(29) Gonzalez, C.; Schlegel, H. B. *J. Chem. Phys.* **1989**, *90*, 2154.
(30) Gonzalez, C.; Schlegel, H. B. *J. Chem. Phys.* **1990**, *94*, 5523.
(31) Frisch, M. J.; et al. *Gaussian 98*; Gaussian Inc.: Pittsburgh, PA, 1998.
(32) Baer, T.; Hase, W. L. *Unimolecular Reaction Dynamics Theory and Experiments*; Oxford University Press: Oxford, 1996.
(33) Garrett, B. C.; Truhlar, D. G. *J. Chem. Phys.* **1979**, *70*, 1593.
(34) Hu, X.; Hase, W. L. *J. Chem. Phys.* **1991**, *95*, 8073.
(35) Miller, W. H.; Handy, N. C.; Adams, J. E. *J. Chem. Phys.* **1980**, *72*, 99.
(36) Baboul, A. G.; Schlegel, H. B. *J. Chem. Phys.* **1989**, *90*, 2154.
(37) Robinson, P. J.; Holbrook, K. A. *Unimolecular Reactions*; Wiley: New York, 1972.
(38) Forst, W. *Theory of Unimolecular Reactions*; Academic: New York, 1973.
(39) Miller, W. H. *J. Am. Chem. Soc.* **1979**, *101*, 6810.
(40) Salem, L. *Electrons in Chemical Reactions*; Wiley: New York, 1982.
(41) Lorquet, J. C.; Leyh-Nihant, B. *J. Phys. Chem.* **1988**, *92*, 4778.
(42) Lorquet, J. C. In *The Structure, Energetics and Dynamics of Organic Ions*; Baer, T., Ng, C. Y., Powis, I., Eds.; Wiley: New York, 1996.
(43) Yarkony, D. R. In *Modern Electronic Structure Theory*; Yarkony, D. R., Ed.; World Scientific: Singapore, 1995.
(44) Harvey, J. N. In *Computational Organometallic Chemistry*; Cundari, T. N., Ed.; Marcel Dekker Inc., New York, 2001; p 291.
(45) Schwarz, H. *Int. J. Mass Spectrom.* **2004**, *237*, 75 and references therein.
(46) Bearpark, M. J.; Robb, M. A.; Schlegel, H. B. *Chem. Phys. Lett.* **1994**, *223*, 26
(47) Faradadzel, A.; Dupuis, M. *J. Comput. Chem.* **1991**, *12*, 276.
(48) Koga, N.; Morokuma, K. *Chem. Phys. Lett.* **1985**, *119*, 371.
(49) Harvey, J. N.; Aschi, M.; Schwarz, H.; Koch, W. *Theor. Chem. Acc.* **1998**, *99*, 95.
(50) Aschi, M.; Harvey, J. N. *Phys. Chem. Chem. Phys.* **1999**, *1*, 5555.
(51) S. Koseki, M. W.Schmidt, M. S. Gordon *J. Phys. Chem.* **1992**, *96*, 10768.
(52) Delos, J. B.; Thorson, W. R. *Phys. Rev. A* **1972**, *6*, 728.
(53) Delos, J. B. *J. Chem. Phys.* **1973**, *59*, 2365.
(54) Pilling, M. J. *Annu. Rev. Phys. Chem.* **1996**, *47*, 81.